J Appl Electrochem (2010) 40:445–456
DOI 10.1007/s10800-009-0015-z

ORIGINAL PAPER

Adsorption, synergistic inhibitive effect and quantum chemical studies of ampicillin (AMP) and halides for the corrosion of mild steel in H_2SO_4

Nnabuk O. Eddy · Eno E. Ebenso · Udo J. Ibok

Received: 21 February 2009 / Accepted: 25 September 2009 / Published online: 10 October 2009

Abstract The corrosion inhibition of ampicillin (AMP) and its synergistic combination with halides (KI, KCl and KBr) for the corrosion of mild steel in H_2SO_4 have been investigated using gravimetric, gasometric, thermometric and infrared (IR) methods. The inhibition efficiencies of AMP for the corrosion of mild steel increased with increase in concentration but decreased with rise in temperature. The adsorption of AMP on the mild steel surface was found to obey the Langmuir adsorption isotherm model. The combination of AMP with the halides (KI, KBr and KCl) enhanced the inhibition efficiency and adsorption behavior of the inhibitor indicating synergism. The inhibition efficiency of AMP increased with increasing concentration and the adsorption of the inhibitor was spontaneous. Physical adsorption mechanism has been proposed from the thermodynamic data obtained. There was a significant correlation between the inhibition efficiency of AMP and some quantum chemical parameters ($R^2 = 0.96$) using the quantitative structure–activity relationship (QSAR) method. Some quantum chemical parameters and the Mulliken charge densities on the optimized structure of AMP were calculated using the B3LYP/6-31G (d,p) basis set method to provide further insight into the mechanism of the corrosion inhibition process.

Keywords Corrosion inhibition · Ampicillin · Halides · Synergism · Adsorption · Quantum chemical calculation · QSAR · B3LYP/6-31G (d,p)

N. O. Eddy (✉)
Department of Chemistry, Ahmadu Bello University, Zaria, Nigeria
e-mail: nabukeddy@yahoo.com; nabukeddy@gmail.com

E. E. Ebenso
Department of Chemistry, North West University (Mafikeng Campus), Private Bag X2046, Mmabatho 2735, South Africa

U. J. Ibok
Department of Chemistry, University of Calabar, PMB 1115 Calabar, Nigeria

1 Introduction

The menace due to corrosion of metals in the oil, metallurgical and other industries has been widely acknowledged and several researches have been carried out on the protection of metals against corrosion. The results obtained revealed that one of the best methods involves the use of inhibitors [1–8].

An inhibitor is a substance that retards the rate of corrosion of metals when added in minute quantity [9]. Most inhibitors used are synthesized from cheap raw materials, some are chosen from compounds having hetero atoms (N, S, O, P) in their aromatic or long carbon chain [10–12] and others are extracts of natural products [13–17]. In our research group, we have investigated the possibility of using some antibiotics for the inhibition of the corrosion of metals [18, 19]. A few investigations have been reported on the use of antibacterial drugs as corrosion inhibitors by some other research groups. Rhodanine azosulpha drugs have been reported to be corrosion inhibitors for the corrosion of 304 stainless steel in HCl solutions using weight loss and potentiostatic polarization techniques by Abdallah [20]. They inhibited corrosion by parallel adsorption on the surface of steel due to the presence of more than one active centre in the inhibitor. Abdallah [21] also studied some antibacterial drugs viz. ampicillin (AMP), cloxacillin, flucloxacillin and amoxicillin as inhibitors for the corrosion

of aluminium in HCl solutions using hydrogen evolution, weight loss and potentiostat polarization techniques. The inhibition of the corrosion of mild steel in HCl solution by four sulpha drug compounds viz. sulfaguanidine, sulfamethazine, sulfamethoxazole and sulfadiazine was reported using both weight loss and galvanostatic polarization [22]. The sulfa drugs have a large number of functional adsorption centres (e.g. $–NH_2$ group, $–SO_2–NH–$ group, O and/or N heteroatoms and aromatic rings). They are strongly basic and are readily soluble in acidic medium. Rhodanine has also been reported to be a corrosion inhibitor for mild steel in HCl by Solmaz et al. [23].

Most of the drugs used play important roles in biological reactions because of their anticonvulsant, antibacterial, antidiabetic, inhibitive to *Mycobacterium tuberculosis* and other properties [24, 25]. The choice of some of the drugs used as corrosion inhibitors is based on the following:

(a) The molecules have oxygen, nitrogen and sulphur as active centres.
(b) They are healthy and reportedly very important in biological reactions (i.e. non-hazardous and environmentally friendly).
(c) They are biodegradable.
(d) They can be easily produced and purified.

Several attempts have been made to predict corrosion inhibition efficiency using a number of individual parameters obtained through quantum chemical calculation methods [26–29]. These trials were aimed at finding possible correlations between corrosion inhibition efficiency and some quantum molecular properties such as dipole moment, energies of the highest occupied (E_{HOMO}) and lowest unoccupied (E_{LUMO}) molecular orbitals and the difference between them (LUMO–HOMO gap), Mulliken charges as well as some structural parameters. We have also recently reported some studies using some drugs as corrosion inhibitors in our laboratories [30–32].

Our present research is aimed at investigating inhibitive and adsorption properties of AMP and halides for the corrosion of mild steel in H_2SO_4 solutions. Some quantum chemical calculations shall be carried out to determine the possible active center(s) responsible for the adsorption of AMP on the mild steel surface. This will give further insight into the adsorption mechanism of the corrosion process. AMP is a beta-lactam antibiotic that has been used extensively to treat bacterial infections since 1961. It is considered as part of the aminopenicillin family and is roughly equivalent to amoxicillin in terms of spectrum and level of activity. It can sometimes result in non-allergic reactions that range in severity from a rash (e.g. patients with mononucleosis) to potentially lethal anaphylaxis [8]. The chemical structure of AMP is as shown below. From the structure, it can be seen that ampicillin {7-(2-amino-2-phenyl-acetyl) amino-3,3-dimethyl-6-oxo-2-thia-5-azabicyclo-[3,2,0]heptane-4-carboxylic acid} has hetero atoms in their heterocyclic structure and it is therefore expected to be a good corrosion inhibitor.

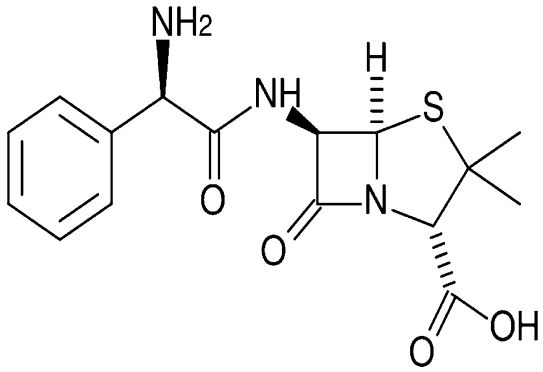

2 Experimental techniques

2.1 Materials

The materials used for the study were mild steel sheet of composition (wt%): Mn (0.6), P (0.36), C (0.15) and Si (0.03) and the rest Fe. The sheet was mechanically pressed cut into different coupons, each of dimension 5 × 4 × 0.11 cm. Each coupon was degreased by washing with ethanol, dipped in acetone and allowed to dry in air before they were preserved in a desiccator. All reagents used for the study were Analar grade and double distilled water was used for their preparation.

The inhibitor (AMP) was supplied by LIVEMOORE Pharmaceutical Company, Ikot Ekpene, Akwa Ibom State, Nigeria, and was used without further purification. The range for the concentrations of the inhibitors used for the study was 3×10^{-4} to 13×10^{-4} M.

2.2 Gravimetric method

In the gravimetric experiment, a previously weighed metal (mild steel) coupon was completely immersed in 250 mL of the test solution in an open beaker. The beaker was covered and inserted into a water bath maintained at 303 K. After every 24 h, each coupon was withdrawn from the test solution, washed in a solution containing 50% NaOH and 100 g L^{-1} of zinc dust (in order to remove the corrosion product). The washed steel coupon was rinsed in acetone and dried in air. The difference in weight for a period of 168 h was taken as total weight loss. The experiments were repeated at 313, 323 and 333 K, respectively. From the weight loss results, the inhibition

efficiency (%I) of the inhibitor, degree of surface coverage and corrosion rates (CR in g h^{-1} cm^{-2}) were calculated using Eqs. 1, 2, and 3, respectively [33]:

$$\%I = (1 - W_1/W_2) \times 100 \quad (1)$$

$$\theta = 1 - W_1/W_2 \quad (2)$$

$$CR = W/At \quad (3)$$

where W_1 and W_2 are the weight losses (g) for mild steel in the presence and absence of the inhibitor in H_2SO_4 solution, θ is the degree of surface coverage of the inhibitor, A is the area of the mild steel coupon (in cm^2), t is the period of immersion (in hours) and W is the weight loss of mild steel after time, t.

2.3 Gasometric method

Gasometric methods were carried out at 303 K as described in the literature [16]. From the volume of hydrogen evolved per minute, inhibition efficiencies were calculated using Eq. 4.

$$\%I = \left(1 - \frac{V_{Ht}^1}{V_{Ht}^0}\right) \times 100 \quad (4)$$

where V_{Ht}^1 and V_{Ht}^0 are the volumes of H_2 gas evolved at time t for inhibited and uninhibited solutions, respectively.

2.4 Thermometric method

This was also carried out as reported elsewhere [21]. From the rise in temperature of the system per minute, the reaction number (RN) was calculated using Eq. 5:

$$RN\ (^\circ C\,min^{-1}) = \frac{T_m - T_i}{t} \quad (5)$$

where T_m and T_i are the maximum and initial temperatures, respectively, and t is the time (min) taken to reach the maximum temperature. The inhibition efficiency (%I) of the inhibitor was evaluated from percentage reduction in the reaction number as follows:

$$\%I = \frac{RN_{aq} - RN_{wi}}{RN_{aq}} \times 100 \quad (6)$$

where RN_{aq} is the reaction number in the absence of inhibitors (blank solution) and RN_{wi} is the reaction number of the H_2SO_4 containing the inhibitors.

2.5 Infrared (IR) analysis

IR analysis of AMP and that of the corrosion products (in the absence and presence of AMP) was carried out using BUCK model 500M infrared spectrophotometer. The sample was prepared using KBr and analysis was carried out by scanning the sample through a wave number range of 400 to 4000 cm^{-1}.

2.6 Quantum chemical calculations

The molecular sketch of AMP was obtained using the GaussView 3.0. All the quantum calculations were performed with complete geometry optimization using standard Gaussian03 (Review B.05) software package [34]. The quantum chemical parameters were calculated using the density functional theory (DFT) method at the level of B3LYP/6-31G (d,p). The following quantum chemical parameters were considered: the energy of the highest occupied molecular orbital (E_{HOMO}), the energy of the lowest unoccupied molecular orbital (E_{LUMO}), the dipole moment (μ), total negative charge (TNC) on the molecule, intrinsic molecular volume (V_i) and dipolar-polarizability factor (π^*).

3 Results and discussion

3.1 Effect of concentration of AMP

Figure 1 shows the variation of weight loss of mild steel with time for the corrosion of mild steel in 0.1 M H_2SO_4 in the absence and presence of various concentrations of AMP at 303 K. Figure 1 reveals that the weight loss of mild steel in H_2SO_4 increased with increase in the period of immersion but decreased with increase in the concentration of AMP. This suggests that the rate of corrosion of mild steel in H_2SO_4 increases with increase in the period of contact and decreases with increase in the concentration of AMP. At higher temperatures (313, 323 and 333 K), weight losses were found to increase with increase in temperature, indicating that the rate of corrosion of mild steel in 0.1 M H_2SO_4 increases with increase in temperature and that

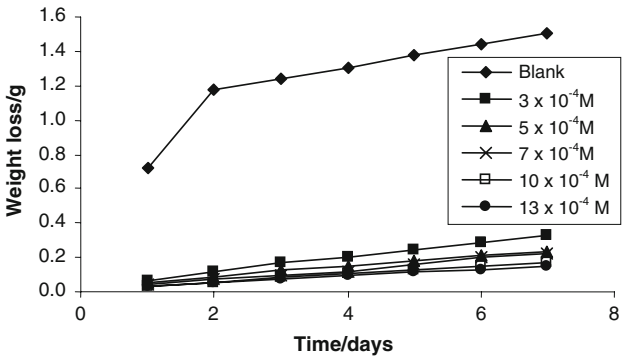

Fig. 1 Variation of weight loss with time for the corrosion of mild steel in 0.1 M H_2SO_4 containing various concentrations of AMP at 303 K

Table 1 Corrosion rates (g cm^{-2} h^{-1}) of mild steel and inhibition efficiencies of AMP for different systems at 303–333 K

$C \times 10^{-4}$ (M)	CR $\times 10^{-4}$ (g cm^{-2} h^{-1})				Inhibition efficiency (%I)					
	303 K	313 K	323 K	333 K	303 K	313 K	323 K	333 K	*T*	*G*
Blank	4.461	4.4811	5.0100	7.1702	–	–	–	–	–	–
3.00	0.9745	2.0272	3.5771	5.0728	78.15	54.75	28.60	29.25	88.00	79.69
5.00	0.6962	1.5738	1.8577	3.4660	84.39	64.87	62.92	51.66	90.40	80.44
7.00	0.6730	0.9471	1.4233	2.8752	84.91	78.86	71.59	59.90	92.80	90.38
10.00	0.5093	0.8911	1.1132	2.3761	88.58	80.11	77.78	66.86	92.80	90.38
13.00	0.4478	0.8543	1.0175	1.7752	89.96	80.93	79.69	75.24	92.80	90.44

T data obtained from thermometric method, *G* data obtained from gasometric method, *CR* corrosion rate

AMP is adsorbed on the surface of mild steel according to the mechanism of physical adsorption [21].

The corrosion rates of mild steel (in the absence and presence of AMP) and inhibition efficiencies of various concentrations of AMP are presented in Table 1. The results obtained show that the rate of corrosion of mild steel decreases with increase in the concentration of AMP but increases with increase in temperature, confirming that AMP is an adsorption inhibitor for the corrosion of mild steel and that a physical adsorption mechanism is applicable for the adsorption of AMP on the surface of mild steel. The inhibition efficiencies obtained from thermometric and gasometric methods were comparable to those obtained from weight loss measurements as indicated by the high correlation coefficients (R^2) of 0.8369 and 0.9062, respectively.

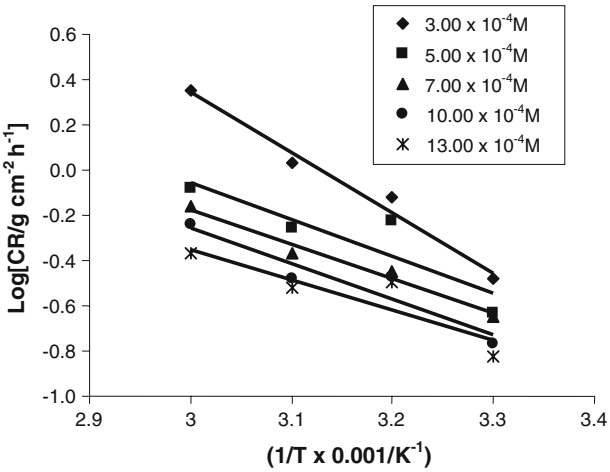

Fig. 2 Plot of log CR versus 1/*T* for the corrosion of mild steel in 0.1 M H_2SO_4 containing various concentrations of AMP

3.2 Effect of temperature

The activation energy for the corrosion of mild steel in 0.1 M H_2SO_4 was calculated using the Arrhenius equation:

$$\mathrm{CR} = A \exp(-E_a/RT) \quad (7)$$

where CR is the corrosion rate of mild steel, *A* is Arrhenius or pre-exponential constant, E_a is the activation energy for the corrosion of mild steel, *R* is the gas constant and *T* is the temperature. The logarithm of both sides of Eq. 7 yields Eq. 8 as:

$$\log \mathrm{CR} = \log A - E_a/2.303RT \quad (8)$$

Plots of log CR versus 1/*T* for the corrosion of mild steel in the presence of various concentrations of AMP yielded straight lines (Fig. 2). From slopes and intercepts of the Arrhenius plot, values of E_a and *A* were computed. The calculated values of E_a ranged from 25.64 to 35.99 kJ mol^{-1} (Table 2). From the results, it is apparent that the activation energies for the corrosion of mild steel in the presence of AMP decreased with increase in the concentration of AMP. The decrease of E_a values with concentrations of AMP is attributed to an appreciable increase in the degree of adsorption of the inhibitor on metal surface with corresponding decrease in reaction rate.

Table 2 Some thermodynamic parameters for the adsorption of AMP on mild steel surface

$C \times 10^{-4}$ (M)	E_a (kJ mol^{-1})	R^2	ΔH_{ads} (kJ mol^{-1})	ΔS_{ads} (J mol^{-1})	R^2
Blank	17.07	0.9634	−69.25	486.16	0.9661
3.00	35.99	0.8832	33.37	−197.60	0.8673
5.00	31.24	0.8036	28.63	−197.60	0.7751
7.00	30.19	0.9728	26.83	−210.19	0.9673
10.00	29.45	0.8921	27.57	−228.55	0.8736
13.00	25.64	0.8055	23.02	−236.28	0.7702

3.3 Thermodynamic and adsorption considerations

The transition state equation (Eq. 9) was used to calculate some thermodynamic parameters (enthalpy of adsorption, ΔH_{ads}, and entropy of adsorption, ΔS_{ads}) for the adsorption of AMP on mild steel surface [1, 19]:

$$\mathrm{CR}/T = R/Nh \times \exp(\Delta S_{ads}/R) \times \exp(\Delta H_{ads}/RT) \quad (9)$$

From the logarithm of both sides of Eq. 9, Eq. 10 is obtained:

$$\log(\mathrm{CR}/T) = \log R/Nh + \Delta S_{ads}/2.303R - \Delta H_{ads}/2.303RT \quad (10)$$

Plots of log (CR/T) versus $1/T$ for AMP were linear. The slopes and intercepts of the transition state plots (Fig. 3) are equal to $-\Delta H_{ads}/2.303R$ and (log $R/Nh + \Delta S_{ads}/2.303R$), respectively. Values of ΔH_{ads} calculated from the slopes of the plots were positive (Table 2), except for the blank solution. ΔH_{ads} values ranged from 23.02 to 33.37 kJ mol^{-1} (mean = 27.88 kJ mol^{-1}), indicating that the adsorption of AMP on mild steel surface is endothermic. Values of ΔS_{ads} calculated from the intercept of the transition state plot were negative (except for the blank) and are presented in Table 2. These values ranged from -197.60 to -236.28 J mol^{-1} (mean = -214.04 J mol^{-1}). The positive and negative values obtained for ΔH_{ads} and ΔS_{ads}, respectively, also indicate that the activated complex may be the rate-determining step and represents association (increasing degree of orderliness) rather than dissociation (disorderliness).

The fact that the inhibition efficiency of different concentrations of AMP increases with increase in concentration suggests that AMP acts as an adsorption inhibitor [10, 33]. Attempts were made to fit data obtained from weight loss measurements into different adsorption isotherms. From the results obtained, the best adsorption isotherm for adsorption

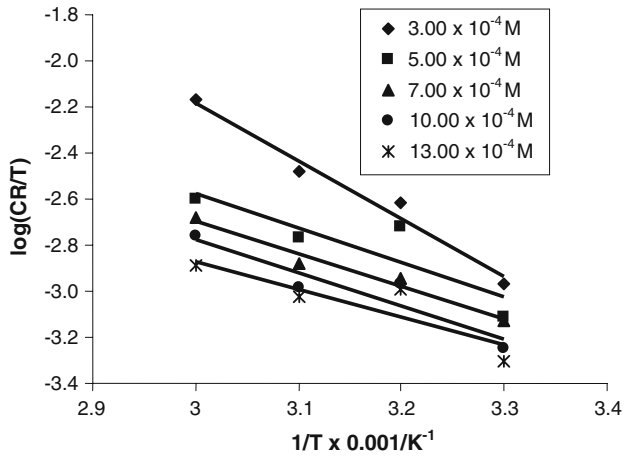

Fig. 3 Plot of log (CR/T) versus $1/T$ for the corrosion of mild steel in 0.1 M H_2SO_4 containing various concentrations of AMP

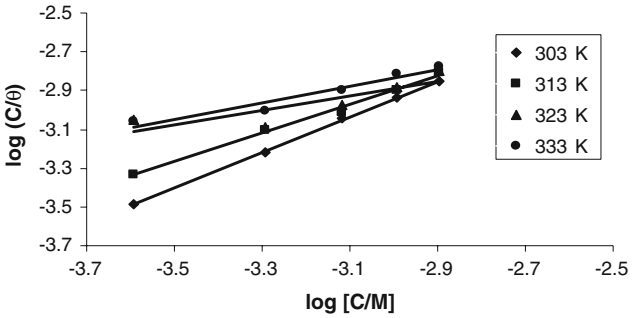

Fig. 4 Langmuir isotherm plot for the adsorption of AMP on the surface of mild steel

of AMP on mild steel surface is Langmuir adsorption isotherm.

Langmuir adsorption equation relates degree of surface coverage to concentration of inhibitor according to Eq. 11 [10]:

$$\log(C/\theta) = \log K + \log C \quad (11)$$

A plot of log(C/θ) versus log C from the weight loss data obtained for AMP yielded straight lines as shown in Fig. 4. The values of some parameters deduced from Langmuir isotherm are presented in Table 3. The results obtained shows that the R^2 values are very close to unity, indicating strong adherence to Langmuir adsorption isotherm.

The free energy of adsorption of AMP on the surface of mild steel is related to the equilibrium constant of adsorption according to Eq. 12 [35–37]:

$$\log K_{ads} = -1.744 - \Delta G_{ads}/2.303RT \quad (12)$$

where K_{ads} is the adsorption equilibrium constant. Table 3 also presents values of ΔG_{ads} calculated from values of K_{ads}, obtained from Langmuir adsorption isotherm. These values are negative and are less than the threshold value of -40 kJ mol^{-1}, indicating that the adsorption of AMP on the surface of mild steel is spontaneous and supports the mechanism of physical adsorption [38–43].

3.4 IR study

Figure 5 shows the IR spectrum of the corrosion product. Figures 6 and 7 show the IR spectrum of AMP and mild steel corrosion product (in the presence of AMP),

Table 3 Langmuir adsorption parameters for the adsorption of AMP on the surface of mild steel

Temperature (K)	log K	Slope	ΔG_{ads} (kJ mol^{-1})	R^2
303	0.1993	0.1993	−11.25	0.9997
313	0.6878	0.6878	−14.55	0.9992
323	1.5449	1.5449	−20.94	0.9397
333	1.7842	1.7842	−21.80	0.9124

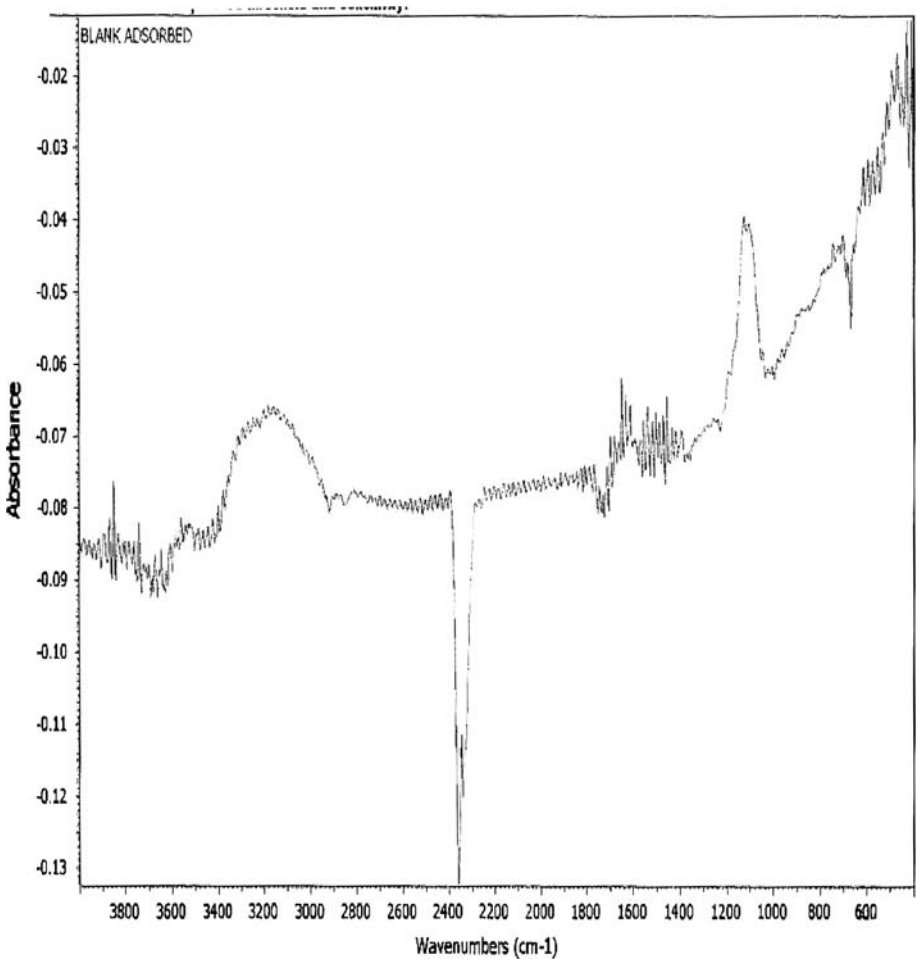

Fig. 5 IR spectrum of the corrosion product of mild steel (without the inhibitor)

respectively. The results (Figs. 6 and 7) reveal that AMP and the mild steel corrosion product (in the presence of AMP) are IR active. The wave numbers and peaks of IR adsorption are recorded in Table 4. From the results, it can be seen that the C–O bond at 2092.85 cm^{-1} was shifted to 2091.30 cm^{-1}, the –NH bond at 1600.78 cm^{-1} was shifted to 1619.58 cm^{-1} but the –OH bond (due to carboxylic acid) was missing in the spectrum of the corrosion product, indicating that there is interaction between the surface of mild steel and AMP and that the adsorption of AMP on the surface of mild steel must have occurred through the missing bond [12]. Also, the –OH bond due to hydrogen bond was found in the spectrum of the corrosion product.

3.5 Synergistic study

The synergism parameter, S_1, was calculated using the relation initially given by Aramaki and Hackerman and reported elsewhere [44–46]:

$$S_1 = \frac{1 - I_{1+2}}{1 - I'_{1+2}} \tag{13}$$

where $I_{1+2} = (I_1 + I_2)$; I_1 is the inhibition efficiency of the halides; I_2 is the inhibition efficiency of AMP; I' is the measured inhibition efficiency for the AMP in combination with halides. S_1 approaches 1 when no interaction between the inhibitor compounds exists, while $S_1 > 1$ points to a synergistic effect. When $S_1 < 1$, the antagonistic interaction prevails, this may be attributed to competitive adsorption. In order to validate Eq. 13 for our study, synergistic studies were carried out between fixed concentration of halides (0.06 M) and various concentrations of the inhibitor (AMP). Values of S_1 for different concentrations of AMP in combination with halides ions are given in Table 5. S_1 values in Table 5 are more than unity, suggesting that the enhanced inhibition efficiency caused by the addition of halide ions to AMP is only due to synergistic effect.

The joint adsorption of AMP and halides on the mild steel surface was found to occur according to Langmuir adsorption isotherm (Fig. 8). The plots of $\log(C/\theta)$ versus $\log C$ yielded straight lines, confirming the application of Langmuir adsorption isotherm to the joint adsorption of AMP and halides on mild steel surface. The adsorption parameters deduced from the Langmuir plots are presented

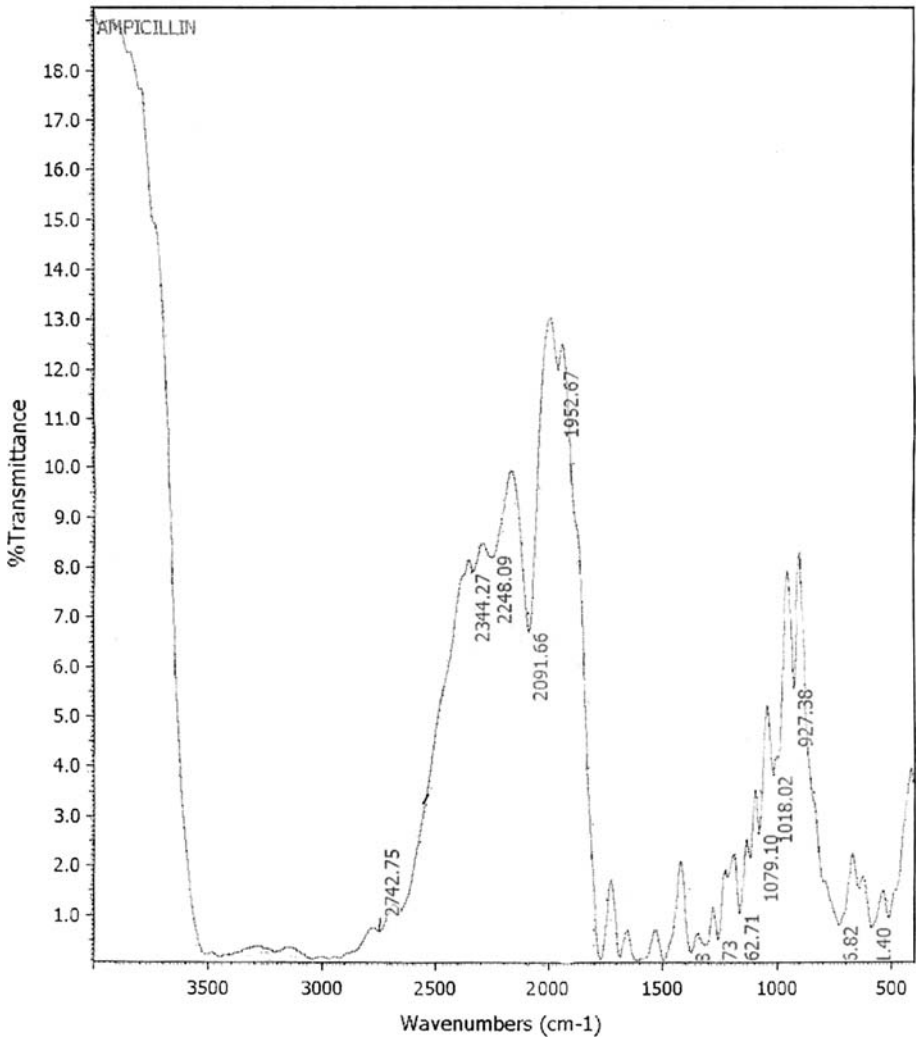

Fig. 6 IR spectrum of pure sample of AMP

in Table 6. The results indicate that the R^2 values for joint adsorption of AMP and halides are much closer to unity than those obtained for AMP alone (Table 3), indicating that there is an improvement in the adsorption behavior of AMP due to synergistic combination of the halides. The slopes of the plots in Figs. 4 and 8 show deviation from unity, indicating non-ideal simulating [47], unexpected from the Langmuir adsorption isotherm. This may be due to the interactions between the adsorbed species on the mild steel surface [48, 49]. It has been postulated in the derivation of the Langmuir isotherm equation that the adsorbed molecules do not interact with one another, and this may not be true for organic molecules having polar atoms or groups which are adsorbed on the cathodic and anodic sites of the metal surface. Such adsorbed species may interact by mutual repulsion or attraction. It is also possible for inhibitor molecules to be adsorbed on anodic and cathodic sites, leading to deviation from unity of the gradient.

The values of the constant (K) obtained from the intercepts of the adsorption plots were used to calculate the free energies of adsorption using Eq. 12. Calculated values of ΔG_{ads} at 303 and 333 K (Table 6) are comparable to those obtained when AMP was used alone. These values were also found to be negative and less than -40 kJ mol^{-1}, indicating that the joint adsorption of AMP and halides is spontaneous and also supported the mechanism of physical adsorption.

In order to calculate the heat of adsorption (Q_{ads}) for the combination of AMP with halides (KBr, KCl and KI), Eq. 14 was used [10]:

$$Q_{ads} = 2.303R\left[\log\left(\frac{\theta_2}{1-\theta_2}\right) - \log\left(\frac{\theta_1}{1-\theta_1}\right)\right] \times \left(\frac{T_2 \times T_1}{T_2 - T_1}\right) \text{kJ mol}^{-1} \quad (14)$$

where θ_2 and θ_1 are degrees of surface coverage at temperatures of 333 K (T_2) and 303 K (T_1), respectively. R is the gas constant. Values of some thermodynamic parameters for the joint adsorption of AMP and halides are presented in Table 7. The values (Q_{ads}) are negative for all

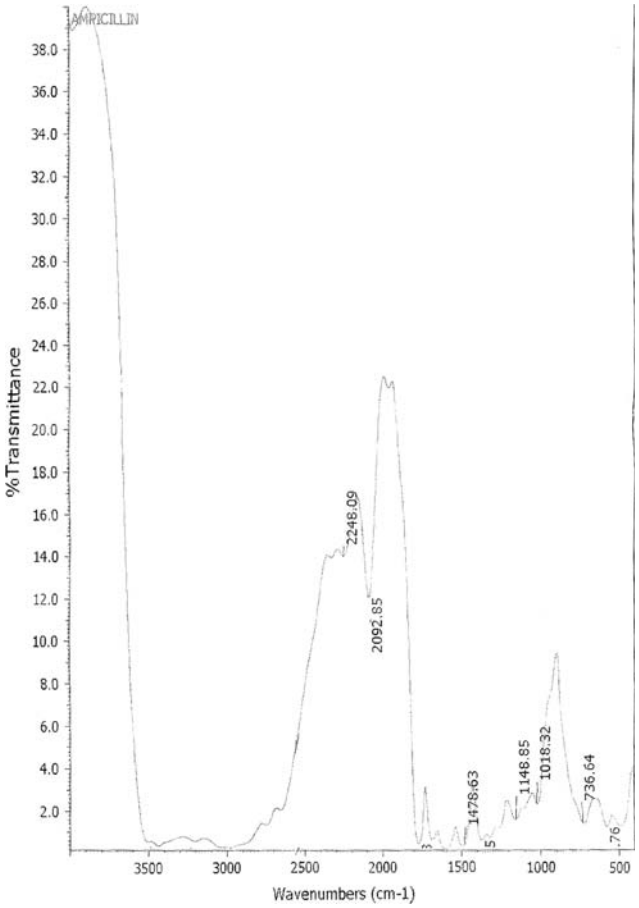

Fig. 7 IR spectrum of the corrosion product of mild steel containing AMP in 0.1 M H_2SO_4

combinations of inhibitors with the halides, indicating that the adsorption is exothermic.

The activation energies for the corrosion of mild steel in the presence of a combination of AMP and halides (KI, KBr and KCl) were calculated using the logarithm form of Arrhenius equation (Eq. 15):

$$\log \frac{CR_2}{CR_1} = \frac{E_a}{2.303R}\left(\frac{1}{T_1} - \frac{1}{T_2}\right) \quad (15)$$

where E_a is the activation energy, CR_1 and CR_2 are the corrosion rates at the temperatures T_1 (303 K) and T_2 (333 K), respectively. The activation energies calculated from Eq. 15 (Table 7) are lower than those obtained for the inhibition of mild steel corrosion by AMP alone, indicating that the halides lower the energy needed for the adsorption of the inhibitor molecule.

The values of entropy of adsorption (ΔS_{ads}) for the combination of AMP with halides (KI, KBr and KCl) were calculated using Gibbs equation (Eq. 16):

$$\Delta G_{ads} = \Delta H_{ads} - T\,\Delta S_{ads} \quad (16)$$

The calculated values of ΔS_{ads} are also presented in Table 7. These values are positive for all combinations of 0.06 M KBr and 0.06 M KI with AMP but negative for combination of 0.06 M KCl with AMP.

3.6 Quantum chemical studies

In this investigation, quantitative structure–activity relationship (QSAR) has also been used to correlate the

Table 4 Wave numbers of IR adsorption by pure AMP and the corrosion product containing AMP as an inhibitor

Pure AMP		Corrosion product (containing AMP)	
Wave number (cm^{-1})	Assignment	Wave number (cm^{-1})	Assignment
3038.85	–OH stretch	3476.79	–OH stretch, H-bonded
2092.85		2091.30	
1771.88			
1600.78	–NH bend	1619.58	–NH bend
1372.65	–C–H rock		
575.76	C–Cl stretch, C–Br stretch	580.92	C–Cl stretch, C–Br stretch

Table 5 Inhibition efficiency and synergistic parameters for various concentrations of AMP in combination with 0.06 M KI, KCl and KBr at 303 and 333 K

$C \times 10^{-4}$ (M) of AMP	KBr (303 K)		KI (303 K)		KCl (303 K)		KBr (333 K)		KI (333 K)		KCl (333 K)	
	IE	S_1	IE	S_1	IE	S_1	IE	S_1	IE	S_1	IE	S_1
3.00	94.63	3.74	86.88	1.00	97.23	3.03	86.30	6.20	55.41	1.00	77.24	3.68
5.00	95.50	1.72	90.89	1.00	97.69	7.91	86.30	6.63	70.63	1.00	87.63	6.67
7.00	95.23	1.32	92.05	1.00	98.04	8.19	87.87	6.71	71.78	1.00	87.03	6.93
10.00	96.43	1.00	93.52	1.00	98.40	8.37	91.99	8.39	76.56	1.31	88.40	6.97
13.00	96.78	1.00	95.37	1.20	98.55	9.62	92.05	9.74	78.56	1.80	88.45	7.08

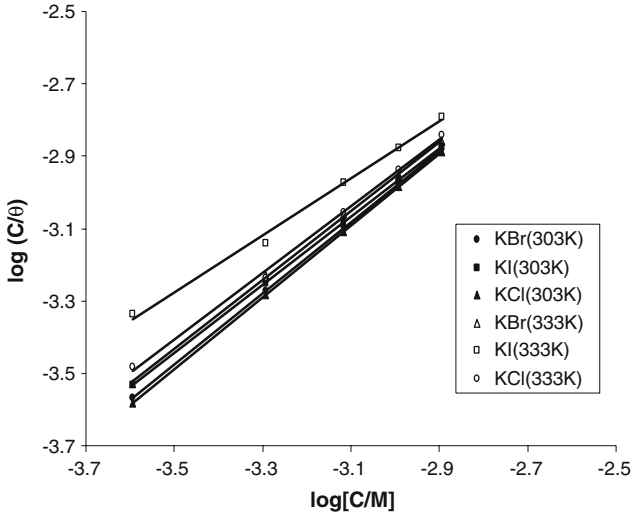

Fig. 8 Langmuir isotherm plot for joint adsorption of AMP and halides on the surface of mild steel

Table 6 Langmuir adsorption parameters for joint adsorption of AMP and 0.06 M halides on the surface of mild steel

AMP + 0.06 M halides	log K	Slope	ΔG_{ads} (kJ mol^{-1})	R^2
KBr (303 K)	0.9869	0.0227	−10.23	1.0000
KI (303 K)	0.9451	0.1367	−10.89	0.9999
KCl (303 K)	0.9914	0.0184	−10.20	1.0000
KBr (333 K)	0.9554	0.0905	−11.67	0.9993
KI (333 K)	0.7903	0.512	−14.36	0.9943
KCl (333 K)	0.9197	0.1879	−12.29	0.9977

inhibition efficiency of the studied inhibitor and its molecular structure. An attempt to correlate the quantum chemical parameters with the experimental %I efficiencies showed that there was no simple relation or no direct trend relationship can be derived from the inhibition performance of AMP using only one method. Although a number of satisfactory correlations have been reported by other investigators [50–56] between the inhibition efficiency of inhibitors used and some quantum chemical parameters, a composite index and a combination of more than one parameter [57] have been used to perform QSAR which might affect the inhibition efficiency of AMP. Therefore, for this study, parameters relevant to the activity of the inhibitor (AMP) under investigation were used for the

Table 7 Values of some thermodynamic parameters for the joint adsorption of AMP and potassium halides on the surface of mild steel

	KBr + AMP	KI + AMP	KCl + AMP
E_a (kJ mol^{-1})	16.22	6.52	17.16
Q_{ads} (kJ mol^{-1})	−23.81	−56.33	−53.59
ΔS_{ads} (J mol^{-1})	110.41	212.29	−140.80

correlation. The linear model approximates inhibition efficiency (IE_{cal} %) as depicted by Eq. 17:

$$IE_{cal} = Ax_jC_i + B \tag{17}$$

where IE_{cal} is the inhibition efficiency, A and B are the regression coefficients determined by regression analysis, x_j is a characteristic quantum index for the inhibitor molecule and C_i denotes the experiment's concentration of the inhibitor. Such linear approach was not found to be satisfactory for the correlation of the present results. Consequently, the non-linear model (NLM) proposed by Lukovits et al. [51] (Eq. 18) and also used by Khaled [57] for studying the interaction of corrosion inhibitors with metal surfaces in acidic solutions has been employed:

$$IE_{cal}\,(\%) = \frac{(Ax_j + B)C_i}{1 + (Ax_j + B)C_i} \times 100 \tag{18}$$

where IE_{cal} (%) is the inhibition efficiency, A and B are the regression coefficients determined by regression analysis, x_j is a quantum chemical index characteristic for the molecule (j) and C_i denotes the experimental concentration i. In the non-linear method of analysis, multiple regressions were performed on the inhibition efficiencies of AMP and a non-linear equation proposed from the B3LYP/6-31G (d,p) method (Eq. 19) gave a good correlation ($R^2 = 0.96$):

$$IE_{cal}\,(\%) = \frac{(-21.36 + 0.277 \times V_i + 314.03 \times E_{LUMO} + 4.02 \times \mu + 1.01 \times TNC) \times C_i \times 100}{(1 + (-21.36 + 0.277 \times V_i + 314.03 \times E_{LUMO} + 4.02 \times \mu + 1.01 \times TNC) \times C_i)} \tag{19}$$

where x_j in Eq. 18 represents a composite index of selected quantum parameters [the energy of the lowest unoccupied molecular orbital (E_{LUMO}), the dipole moment (μ), total negative charge (TNC) and the LSER parameter, intrinsic molecular volume, V_i] (presented in Table 8).

The effectiveness of an inhibitor can be related to its spatial molecular structure, as well as their molecular electronic structure [58]. Also, there are certain quantum chemical parameters that can be related to the metal–inhibitor interaction namely E_{HOMO}, E_{LUMO}, $\Delta E = E_{LUMO} - E_{HOMO}$, dipole moment, μ etc. E_{HOMO} is often

Table 8 Quantum chemical parameters of AMP using gas phase B3LYP/6-31G (d,p)

V_i (cm^3 M^{-1})	π^*	E_{HOMO} (eV)	E_{LUMO} (eV)	$E_{LUMO-HOMO}$ (eV)	μ (Debye)	TNC
4.07	3.72	−0.2178	−0.0420	0.176	1.0579	−5.612

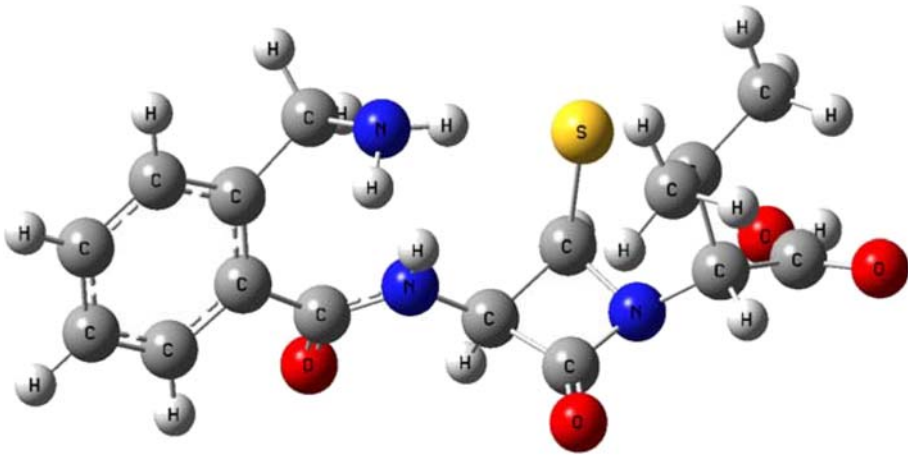

Fig. 9 Optimized structure of AMP

associated with the capacity of a molecule to donate electrons and an increase in the value of E_{HOMO} can facilitate the adsorption and therefore the inhibition efficiency by indicating the disposition of the molecule to donate orbital electrons to an appropriate acceptor with empty molecular orbital. In the same way, low values of the energy gap, $\Delta E = E_{LUMO} - E_{HOMO}$ will yield good inhibition efficiencies, because the energy needed to remove an electron from the last occupied orbital will be low [59]. Similarly, low values of the dipole moment, μ, will favor the accumulation of inhibitor molecules on the metallic surface [59]. The optimized structure of AMP is shown in Fig. 9 and the HOMO and LUMO diagrams of AMP are shown in Figs. 10 and 11. Figures 10 and 11 show that the most susceptible sites for electrophillic attack occur at the nitrogen and oxygen atoms. Figure 12 shows the Mulliken charge densities calculated from the optimized geometry of AMP using the B3LYP/6-31G (d,p) method. The results of some of the quantum chemical parameters calculated are presented in Table 8. The results seem to indicate that both values of the energy gap, $\Delta E = E_{LUMO} - E_{HOMO}$, as well as that of the dipole moment, μ, favor AMP, implying its effectiveness as a corrosion inhibitor. The negative sign of the E_{HOMO} value obtained and other thermodynamic parameters indicate that the data obtained support physical adsorption mechanism. Also, from the molecular orbital density distribution of AMP, it is observed that the electron densities of the frontier orbitals are well proportioned. This type of structure is difficult to form chemically bond active centres and point to the fact that the physical adsorption mechanism occurred by π-stacking between the interaction sites [32].

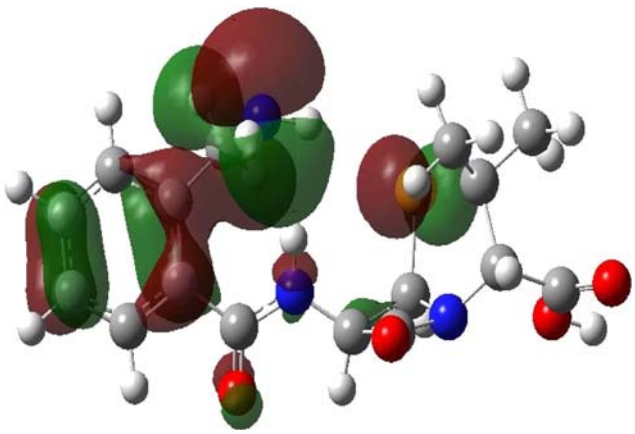

Fig. 10 HOMO of AMP using B3LYP/6-31G (d,p)

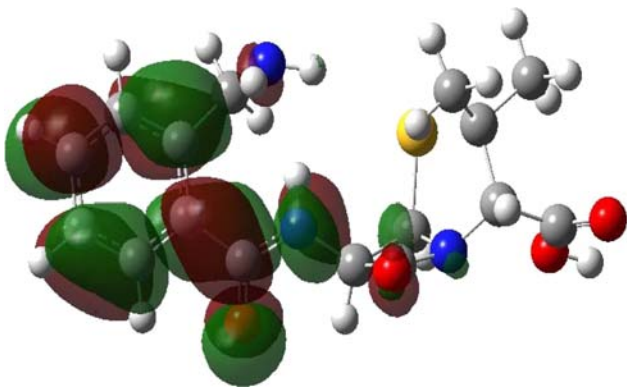

Fig. 11 LUMO of AMP using B3LYP/6-31G (d,p)

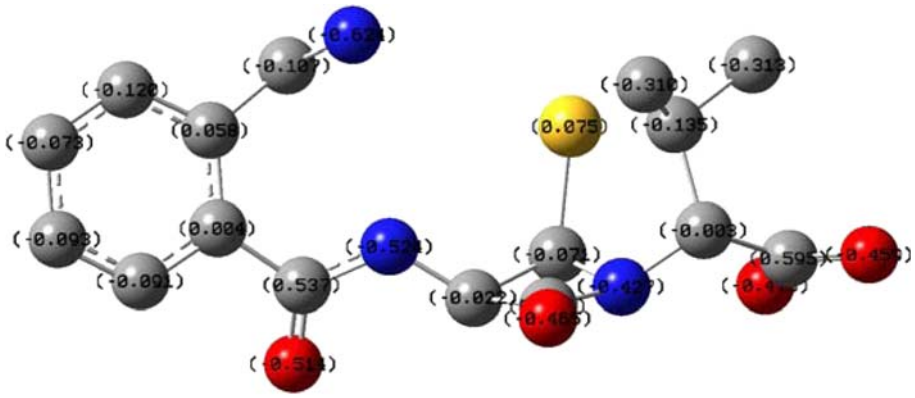

Fig. 12 Mulliken charges on the optimized structure of AMP using B3LYP/6-31G (d,p)

The use of Mulliken population analyses to probe adsorption centres of inhibitors has been widely reported [60–63]. There is a general consensus by several researchers that the more negatively charged a heteroatom is, the more it can be adsorbed on the metal surface through the donor–acceptor type reaction [64–66]. It has also been reported that electrophiles attack molecules at sites of negative charge [67], which means that from the values of Mulliken charges in Fig. 12, it is possible to assume that all the nitrogen atoms present a considerable excess of negative charge −0.62, −0.52 and −0.47 and negative charges around most carbon atoms of the aromatic rings. Similar observation can be made for the oxygen atoms. Therefore, AMP molecule can be adsorbed on the mild steel surface using these active centres (N and O) leading to corrosion inhibition.

4 Conclusions

1. AMP was found to be a good adsorption inhibitor for the corrosion of mild steel in H_2SO_4.
2. The adsorption of AMP on the mild steel surface follows the Langmuir adsorption isotherm and the inhibition efficiency increased with increase in concentration of the AMP but decreased with rise in temperature suggesting physical adsorption.
3. Addition of halides (KCl, KBr and KI) synergistically increased the inhibition efficiency of AMP and Langmuir adsorption isotherm was also obeyed for AMP combined with the halides.
4. Using QSAR approach, a highly significant correlation coefficient ($R^2 = 0.96$) has been obtained between the inhibition efficiency of AMP with some calculated quantum chemical parameters using the non-linear model of Lukovits et al.
5. Quantum chemical calculations using the B3LYP/6-31G (d,p) revealed that the adsorption of AMP on the mild steel surface may be concentrated around the nitrogen and oxygen atoms as active centres.

References

1. Abdallah M (2004) Portugaliae Electrochim Acta 22:161
2. Anauda L, Sathiyanathan RA, Maruthamuthu SB, Selvanayagam MC, Mohanan SB, Palaniswamy NB (2005) Indian J Chem Technol 12(3):356
3. Ashassi-Sorkhabi H, Shaabani B, Aligholipour B, Seifzadeh D (2006) Appl Surf Sci 252:4039
4. Bendahou MA, Benadellah MBE, Hammouti BB (2006) Pigment Resin Technol 35:95
5. Eddy NO, Odoemelam SA, Akpanudoh NW (2008) J Chem Technol 4:1
6. Eddy NO, Ekwumemgbo P, Odoemelam SA (2008) Int J Phys Sci 3:1
7. Ebenso EE, Ibok UJ, Ekpe UJ, Umoren SA, Ekerete J, Abiola OK, Oforka NC, Martinez S (2004) Trans SAEST 39:117
8. Eddy NO (2008) Inhibition of corrosion of mild steel by some antibiotics. Ph.D. Thesis, University of Calabar, p 234
9. Eddy NO, Ebenso EE (2008) Afr J Pure Appl Chem 2:1
10. Ebenso EE, Eddy NO, Odiongenyi AO (2008) Afr J Pure Appl Chem 2:107
11. Chetounani A, Hammouti BB, Benkaddour M (2004) Pigment Resin Technol 33:26
12. Eddy NO, Odoemelam SA, Odiongenyi AO (2008) J Appl Electrochem 39:849
13. Bouyanzer A, Hammouti BB (2004) Pigment Resin Technol 33:287
14. El-Etre AY (2003) Corros Sci 45:2485
15. El-Etre AY (2006) Appl Surf Sci 252:8521
16. El-Etre AY, Abdallah M, El-Tantawy ZE (2005) Corros Sci 47:385
17. Eddy NO, Odoemelam SA (2009) Pigment Resin Technol 38:111
18. Odoemelam SA, Eddy NO (2008) J Surf Sci Technol 24:1
19. Odoemelam SA, Eddy NO (2008) J Mater Sci 4:1
20. Abdallah M (2002) Corros Sci 44:717
21. Abdallah M (2004) Corros Sci 46:1981
22. El-Naggar MM (2007) Corros Sci 49(5):2226
23. Solmaz R, Kardas G, Yazici B, Erbil M (2005) Prot Met 41:581
24. Sing WT, Lee CL, Yeo SL, Lim SP, Sim MM (2001) Bioorg Med Chem Lett 11:91
25. El-Dissouky A, El-Bindary AA, El-Soubati AZ, Hilali AS (2001) Spectrochim Acta A 57:1163
26. Ozcan M, Karadag F, Dehri I (2008) Colloids Surf A 316:55
27. Bereket G, Ogretir C, Ozsahim C (2004) J Mol Struct (Theochem) 66:173
28. Li Y, Zhao P, Liang Q, Hou B (2005) Appl Surf Sci 252:1245
29. Ogretir C, Mihci B, Bereket G (1999) J Mol Struct (Theochem) 488:223

30. Ebenso EE, Eddy NO, Odiongeyi AO (2009) Portugaliae Electrochim Acta 27:13
31. Odoemelam SA, Ogoko EC, Ita BN, Eddy NO (2009) Portugaliae Electrochim Acta 27:57
32. Arslan T, Kandemirli F, Ebenso EE, Love I, Alemu H (2009) Corros Sci 51:35
33. Eddy NO, Odoemelam SA, Ekwumemgbo P (2009) Sci Res Essay 4:033
34. Frisch MJ, Trucks GW, Schlegel HB, Scuseria GE, Robb MA, Cheeseman JR, Zakrzewski VG, Montgomery JA, Stratmann RE, Burant JC, Dapprich S, Millam JM, Daniels AD, Kudin KN, Strain MC, Farkas O, Tomasi J, Barone V, Cossi M, Cammi R, Mennucci M, Pomelli C, Adamo C, Clifford S, Ochterski J, Petersson GA, Ayala PY, Cui Q, Morokuma K, Malick DK, Rabuck AD, Raghavachari K, Foresman JB, Cioslowski J, Ortiz JV, Baboul AG, Stefanov B, Liu G, Liashenko A, Piskorz P, Komaromi I, Gomperts R, Martin RL, Fox AJ, Keith T, Al-Laham MA, Peng CY, Nanayakkara A, Challacombe M, Gill PMW, Johnson B, Chen W, Wong MW, Andres JL, Gonzalez C, Head-Gordon M, Replogle ES, Pople GA (1998) Gaussian 98. Revision A.7. Gaussian Inc., Pittsburgh, PA
35. Essa MC, Maruthamuthu SB, Selvanayagam MA, Palaniswamy NB (2005) J Indian Chem Soc 2:357
36. Yurt A, Bereket G, Kivrak A, Balaban A, Erk B (2005) J Appl Electrochem 35:1025
37. Fouda AS, Heakal FE, Radwan MS (2009) J Appl Electrochem 39:391
38. Rajappa SK, Venkatesha TV, Peaveen BM (2008) Bull Mater Sci 31:37
39. Ebenso EE (2003) Mater Chem Phys 79:58
40. Ebenso EE (2003) Bull Electrochem 19:209
41. Ebenso EE (2004) Bull Electrochem 20:55
42. Bhajiwala HM, Vashi RT (2001) Bull Electrochem 17:441
43. Bilgic S, Sahin M (2001) Mater Chem Phys 70:290
44. Umoren SA, Ogbobe O, Ebenso EE (2006) Bull Electrochem 22:155
45. Oguzie EE, Okolue BN, Ebenso EE, Onuoha GN, Onuchukwu AI (2004) Mater Chem Phys 87:394
46. Gomma GK (1998) Mater Chem Phys 55:241
47. Badawy WA, Ismail KM, Fathi AM (2006) Electrochim Acta 51:4182
48. Migahed MA, Mohammed HM, Al-Sabagh AM (2003) Mater Chem Phys 80:169
49. Azim A, Shalaby LA, Abbas H (1974) Corros Sci 14:21
50. Costa JM, Lluch JM (1984) Corros Sci 24:924
51. Lukovits I, Kalman E, Palinkas G (1995) Corrosion 51:201
52. Sastri VS, Perumareddi JR (1997) Corrosion 53(18):617
53. Li SL, Wang YG, Chen SH, Yu R, Lei SB, Ma HY, Liu De X (1999) Corros Sci 41:1769
54. Bereket G, Hur E, Ogretir C (2002) J Mol Struct (Theochem) 578:79
55. Cruz J, Garcia-Ochoa E, Castro M (2003) J Electrochem Soc 150:B26
56. Wang D, Li S, Ying Y, Wang M, Xiao H, Chen Z (1999) Corros Sci 41:1911
57. Khaled KF (2006) Appl Surf Sci 252:4120
58. Ashassi-Sorkhabi H, Shaabani B, Seifzadeh D (2005) Electrochim Acta 50:3446
59. Khalil N (2003) Electrochim Acta 48:2635
60. Fang J, Li J (2002) J Mol Struct (Theochem) 593:171
61. Hasanov B, Sadikoglu M, Bilgic S (2007) Appl Surf Sci 253:3913
62. Allam NK (2007) Appl Surf Sci 253:4570
63. Kandemirli F, Sagdina S (2007) Corros Sci 49:2118
64. Bereket G, Ogretir C, Ozsahim C (2003) J Mol Struct (Theochem) 663:39
65. Ozcan M, Dehri I, Erbil M (2004) Appl Surf Sci 236:155
66. Li W, He Q, Pei C, Hou B (2007) Electrochim Acta 52:6386
67. Ozcan M, Dehri I, Erbil M (2004) Prog Org Coat 51:181